https://doi.org/10.48047/AFJBS.6.Si4.2024.669-698

African Journal of Biological Sciences

Development and optimization of polyherbal transdermal patch for arthritis: In-vitro and Ex-vivo evaluation

Resa P. Parmar[1*], Niranjan S. Kanaki[2], Khyati N. Shah[3], Pragnesh Patani[4]

[1*]Lecturer, B. K. Mody Government Pharmacy College, Rajkot, Gujarat, India.
[2]Associate Professor, K. B. Institute of Pharmaceutical Education and Research, Gandhinagar, Gujarat, India.
[3]Assistant Professor, Government Pharmacy College, Gandhinagar, Gujarat, India.
[4]Principal and Professor, Khyati college of Pharmacy, Ahmedabad, Gujarat, India.

***Corresponding Author:** Resa P. Parmar
*Lecturer, B. K. Mody Government Pharmacy College, Rajkot, Gujarat, India. : resapparmar@gmail.comMobile No: 9723617300ORCID ID: 0009-0006-0334-7490

Article History

Volume 6, Issue Si4, 2024
Received: 25 May 2024
Accepted: 15 June 2024
doi:
10.48047/AFJBS.6.Si4.2024.669-698

Abstract

The present study is aimed to develop, optimize and evaluate polyherbal transdermal patch consists of boswellic acids, curcuminoids, diosgenin and rutin for treatment of arthritis. Traditionally, these phytochemicals are used in the treatment of arthritis. Matrix type of transdermal patch was formulated by solvent casting method using the combinations of polymers, Eudragit RL 100 and Eudragit RS 100, polyethylene glycol 400 as a plasticizer and l-menthol as a permeation enhancer. A 2^3 full factorial design was applied for the optimization of process variables such as polymers and penetration enhancer concentration. Selected responses were tensile strength and Q24. Patches were evaluated for physicochemical properties like thickness, weight variation, folding endurance, percentage flatness, percentage moisture content, percentage moisture uptake, water vapor transmission rate, drug content, in-vitro diffusion studies and ex-vivo skin permeation studies. All the formulations had desirable physicochemical properties. Formulation P8 showed maximum Q24, So P8 batch was studied further for ex-vivo skin permeation. Kinetic modelling suggested that non-Fickian type of diffusion is dominant mechanism for drug release. No erythema or edema was observed in the skin irritation test confirming the patch was non-toxic and safe. Stability studies were carried out according to ICH guidelines which clearly revealed that the optimized patch is stable. The formulated transdermal patch could release significant amounts of drugs into the systemic circulation. Polyherbal patch could provide an alternative to traditional NSAIDs for arthritis treatment.

Keywords: Boswellic acid, Curcuminoids, Diosgenin, Rutin, Transdermal patch, Arthritis.

Introduction

Rheumatoid Arthritis (RA) is one of the most common musculoskeletal disease and disorder (Srivastava, 2009). RA is both, a disorder of cell-mediated immunity and an extravascular immune complex disease, leads to chronic inflammation, granuloma formation and joint destruction (Scott et al., 2010). The etiopathogenesis of RA involves diverse and complex factors such as genetic background, rheumatoid factor (autoantibodies), immune complexes, compliment activation,

lymphocytes, arachidonic acid metabolites, free oxygen radicals (Smolen et al., 2016). In allopathic system, treatments include mainly non-steroidal anti-inflammatory drugs (NSAIDs), different classes of disease-modifying anti-rheumatic drugs (DMARDs), corticosteroids and other cell-targeted therapies, including T-, B-, and monocytes/ macrophages-targeted therapies. Different treatments are currently emerging, such as the use of cell-based therapies, including mesenchymal stem cell (MSCs)-based therapy, tolerogenic dendritic cell (tolDCs)-based therapy. However, not all these treatments can be efficient for all patients and their long-term use could lead to serious adverse effects (Mrid et al., 2022). Furthermore, higher cost and negative impacts on health have limited the use of synthetic drugs in arthritic treatment. Of these synthetic medicines, herbal medicines are also gaining popularity for arthritis treatment, due to fewer side effects.

Phytochemicals, agents derived from plants, can modify the expression of pro-inflammatory signals clearly and therefore they have potential against arthritis. (Khanna et al., 2007). These include flavonoids, terpenes, quinones, catechins, alkaloids, anthocyanins and anthoxanthins, all of which are known to have anti-inflammatory effects (Jain et al., 2021). Boswellic acid (BA), a constituent of Boswellia serrata (Family- Burseraceae) showed anti-inflammatory, anti-rheumatic and anti-pyretic activities with no ulcerogenic effect and well tolerated in as high a dose as 2 gm/kg (p.o.) in mice. It improves blood supply to joints and restores integrity of vessels obliterated by spasm of internal damage (Sharma et al., 1989). It is lipophilic in nature and classified as Biopharmaceutical Classification System (BCS) class IV drug due to poor permeability, high first pass metabolism and high frequency of dose requirement (Varia et al., 2022).

Curcumin, a constituent of Curcuma longa (Family-Zingiberaceae) is an effective anti-inflammatory agent with no analgesic and anti-pyretic activity. It is well tolerated in as high a dose as 2 gm/kg (p.o.) in mice (Hatcher et al., 2008). It has been reported to inhibit both lipoxygenase and cyclooxygenase as well as a potent scavenger of oxygen free radicals (Ammon et al., 1993). Curcumin is also classified as BCS class IV molecule based on its poor aqueous solubility (11 ng/ml in aqueous buffer pH 5) and permeability through intestinal epithelial cells (Tonnesen et al., 2002).

Diosgenin, a steroidal sapogenin constituent of Trigonella foenum-graceum (Family-Leguminosae), possesses anti-rheumatic and antiviral properties, suppresses inflammation, inhibits proliferation and induces apoptosis in a variety of tumour cells (Javed et al., 2023). It is often used as a raw precursor in the production of steroidal drugs and hormones such as, glucocorticoids, testosterone and progesterone (Patel et al., 2012). It shows low oral bioavailability due to poor aqueous solubility and strong hydrophobicity (Liu et al., 2017).

Rutin, also called as rutoside or vitamin P, has been used for its phlebotonic properties and capillary protector used for the treatment of haemorrhoids and as antioxidant, anti-inflammatory, cardio-protective, neuroprotective, anti-thrombotic, anti-aging agent and used in multivitamin preparations (Ganeshpurkar and Saluja, 2017). The BCS has classified rutin as a Class II drug, characterized by poor solubility in aqueous environment, yet good in permeability through cellular membrane (Ravi et al., 2018).

Chemical structures of selected phytochemicals are given in Figure no 1.

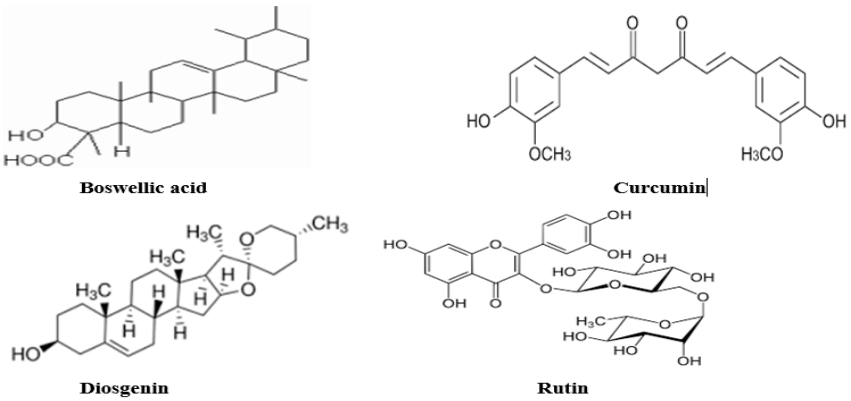

Figure 1: Chemical structure of boswellic acid, curcumin, diosgenin and rutin

These phytochemicals inhibit the inflammatory pathway through different targets. They are classified as BCS class IV and II molecules. Hence, they need to be delivered to the site of action through an alternate route to make the most of their therapeutic efficacy. Moreover, if applied near the joints, larger drug concentration can be achieved near the joints, which are the site of action of the anti-arthritic drugs. Therefore, an attempt was made to formulate these phytochemicals into a Transdermal Drug Delivery System (TDDS). TDDS is a self-contained, discrete dosage form, which when applied to the intact skin, will deliver the drug at a controlled rate to the systemic circulation. TDDS established itself as an integral part of novel drug delivery systems due to many significant advantages over other routes of drug delivery, like target delivery, avoidance of hepatic first-pass metabolism, devoid of gastric irritation, avoid gastric pH effects, gastric emptying rate, devoid of frequent dosing. Varieties of approaches such as transdermal gel, patch, iontophoresis, sonophoresis, electroporation, microneedles, abrasion, microporation, laser radiation, etc. have been designed for the transdermal delivery of the drug (Prausnitz and Langer, 2008).

Amongst the various approaches, transdermal patch is found to be a promising approach in TDDS. It is a medicated patch that can deliver drugs through skin portals directly to the bloodstream at a predetermined rate.it is the most comfortable dosage form as it is non-invasive, avoids the gastrointestinal tract and bypasses first-pass metabolism, can have multiday therapy, and can be terminated at any time (Roy, 2011). Thus, the present study is aimed to develop matrix type polyherbal transdermal patch consisting of traditional used antiarthritic phytochemicals, boswellic acids, curcumin, diosgenin, rutin which can be an alternative to traditional NSAIDs in treating patients with arthritis conditions.

Materials and Methods

Materials

Salai guggul (Oleogum resin of Boswellia serrata) and turmeric powder (Rhizome of Curcuma longa) were purchased from reputed herbal store. Diosgenin and rutin were purchased from Yucca enterprises, Mumbai. Eudragit RL 100 and Eudragit RS 100 were purchased from Seva fine Chemical Ltd, Mumbai. L- menthol was purchased from Lincoln Pharmaceuticals Limited, Ahmedabad. Poly vinyl alcohol, Polyethylene Glycol 400 and phosphate buffer solution (PBS) (pH 5.5) were purchased from S. D. Fine Chemicals, Mumbai. The solvents and agents used for the determination of phytochemical content in the samples by HPTLC method were analytical grade and obtained from Finar chemicals, Ahmedabad. The artificial membrane (MF-Millipore_ membrane filter, filter code VSWP) used for the in-vitro permeation study was purchased from Millipore Corporation (Bedford, MA, USA).

Identification, Collection and Authentication of plant materials

Salai guggul was ground to coarse powder using pulverizer and then stored in airtight container in cool and dry place till further use. Oleogum resin of Boswellia serrata was authenticated by subjected to macroscopic studies which comprised of study of organoleptic characters of the drug viz., color, odour, appearance, taste, smell, texture and fracture. Authentication of Turmeric powder was done by comparing the morphological and microscopical characteristics with those mentioned in literature (GoI 1999 a, b RRL 1998).

Isolation and characterization of Phytochemicals

Boswellic acids were isolated by the method reported by Basur (2005). About 50 gm of gum resin of salai guggul was extracted with methanol. After filtration, the extract was concentrated to a viscous solution. This concentrated solution was dissolved in 100 ml of 10% aqueous potassium hydroxide solution at pH 9-10. The alkali-soluble fraction was separated by filtration and acidified with 10% hydrochloric acid to pH 3-5. The precipitated organic acids were extracted with dichloromethane. The dichloromethane extract was washed with distilled water until the aqueous layer had a neutral pH. The resulting dichloromethane extract was dried over anhydrous sodium sulphate and the solvent was evaporated to obtain a white powder of mixture of boswellic acids. Boswellic acid mixture was characterized by comparing its melting point, Fourier Transform Infrared (FTIR) spectrum and Differential Scanning Calorimetry (DSC) thermogram with those reported in the literature (Fartyal et al., 2011). Curcuminoids were isolated by the method reported by Revathy (2011). About 50 gm of powdered Curcuma longa rhizomes were extracted in a Soxhlet apparatus with 150ml of petroleum ether for 2 hr. Petroleum ether extract was discarded and the marc was re-extracted with methanol for 6 hours. The methanolic extract was then cooled, filtered and concentrated. The concentrated methanolic extract was treated with hexane to remove oil and then extracted with acetone. Acetone soluble fraction was collected and concentrated to dryness to get a dark orange colored mixture of curcuminoids. This crude curcuminoid mixture contained curcumin, demethoxycurcumin and bisdemethoxycurcumin. The curcuminoid fraction was characterized by melting point, FTIR spectroscopy and DSC and comparing these data with those reported in the literature (Mohan et al., 2012). Diosgenin and rutin were characterized by comparing melting point, FTIR spectroscopy and DSC with data reported in the literature (Indrayanto et al., 1994 and Panhwar et al., 2014).

Development of High-Performance Thin Layer Chromatography (HPTLC) methods for analysis of phytochemicals

HPTLC method and Chromatographic conditions

The HPTLC system (Camag, Switzerland) consisted of Linomat V auto sprayer connected to a nitrogen cylinder, a twin trough chamber (10 × 10 cm), a derivatization chamber and a plate heater. Precoated silica gel 60 F254 TLC plates (10 × 10 cm, layer thickness 0.2 mm, E. Merck KGaA, Darmstadt, Germany) were used as stationary phase. TLC plates were prewashed twice with 10 ml of methanol and activated at 80°C for 5 min prior to sample application. Analysis was carried out using TLC scanner III with winCATS software. (V 1.4.6, Camag). The samples and standards were applied onto the plates as a band with 8mm width using a 100-microliter sample syringe (Hamilton, Switzerland) at 10 mm from the bottom of the plate, at a delivery speed of 10 s/µl. The application parameters were identical for all the analysis. Linear ascending development was carried out in a twin trough glass chamber (10 × 10 cm) which was pre-saturated with the mobile phase.

Calibration curve of Phytochemicals

A stock solution of all phytochemicals (1mg/ml) was prepared in methanol. Different volumes of stock solution 1, 2, 3, 4, 5 and 6 µl were spotted on TLC plate to obtain concentrations of 1, 2, 3, 4, 5 and 6 µg per spot of phytoconstituent. Plate was developed in the mobile phase n-hexane: acetone (7:3) at 25 ± 2^{0}C temperature and 40% relative humidity and allowed to travel up to 8 cm distance. After air drying of the plate, spots were visualized in daylight and scanned at 423 nm for curcuminoids. The plate is further derivatized by spraying anisaldehyde sulphuric acid reagent and heating it at 110^{0}C for 5 minutes. The derivatized plate was scanned at 540nm to visualize spots of boswellic acids and diosgenin. For rutin, plate was developed in the mobile phase, ethyl acetate: glacial acetic acid: formic acid: water (100:11:11:25) and scanned at 258nm. The Rf, peak areas and absorption spectra were recorded. Calibration curves were prepared by plotting peak areas versus concentration of the phytochemical (Parmar and Kanaki, 2017, 2018). HPTLC method was developed for all phytochemicals in two different mediums. One medium is methanol solvent which was used for the estimation of drug content. Another medium was diffusion medium, Phosphate Buffer Solution (PBS) of pH 5.5 containing 1% Tween 80, which was used for analysis of these compounds during the drug release study and skin permeation study.

Selection of excipients

Selection of polymers

Preliminary screening was carried out to check the effect of various polymer combinations on transdermal patch formulation. Composition of preliminary trial batches includes polymers like Hydroxy Propyl Methyl Cellulose (HPMC), Ethyl Cellulose (EC), Eudragit RL 100 (ERL 100), Eudragit RS 100 (ERS 100), Poly Vinyl Pyrrolidine K30 (PVP K30). Polymeric films were evaluated based on their thickness, weight, % flatness and folding endurance.

Selection of plasticizers

Plasticizers were selected based on nature, solubility in solvents, polymer combinations and folding endurance of patch. Various plasticizers were tested like propylene glycol, polyethylene glycol 400, castor oil, glycerol, dibutyl phthalate.

Selection of backing membrane

Backing membrane works as a flexible film and provides low water vapour transmission and high oxygen transmission rates. Polyvinyl Alcohol (PVA) is used in the fabrication of transdermal drug delivery systems as the backing membrane. Preliminary trial of backing membrane was done using various concentration of PVA. Based on Water Vapour Transmission Rate (WVTR) and tensile strength, optimum concentration of PVA was selected. WVTR is defined as the quantity of moisture transmitted through unit area of film in unit time. Glass cells were filled with 2 g of anhydrous calcium chloride and a film of specified area was affixed onto the cell rim. The assembly was accurately weighed and placed in a humidity chamber (80 ± 5% RH) at 27 ± 2 °C for 24 hrs. The cell was reweighed and WVTR was determined using following formula.

WVTR = (Final Weight - Initial Weight)/ Area × 24

Selection of permeation enhancers

Permeation enhancers were selected based on nature, solubility in solvents, polymer combinations and percentage of drug release from curcumin patch. Various permeation enhancers were tested like oleic acid, menthol, isopropyl alcohol, propylene glycol.

Drug excipients compatibility study

Drug and excipients were mixed and placed at room temperature for 24 hours. Drug excipients compatibility was checked by FTIR spectroscopy and DSC studies. IR spectra for drug mixture and their mixture with polymers were recorded in a FTIR spectrophotometer with KBr pellets. The scanning range was 400- 4000 cm^{-1}. DSC analysis of the drug mixture and their mixture with polymers were performed by using an automatic thermal analyzer system (Shimadzu DSC-60) to evaluate the drug-polymer interactions. The analysis was performed at a rate of 10°C per min from 50°C to 350°C under a nitrogen flow of 20 ml/min (Patel et al., 2009).

Development of transdermal patch

Backing membrane was prepared by casting 5% aqueous solution of PVA followed by drying at 60° C for 6 hrs. Drug loaded matrix type transdermal patches were prepared by solvent casting method. Petri-dish with total area of 38.465 cm^2 was used. Polymers were accurately weighed and dissolved in dichloromethane: methanol (50:50). The polymeric dispersion was stirred for 2 min to remove entrapped air bubbles. PEG 400 and menthol were added to the polymeric dispersion. Boswellic acids (60 mg/9cm^2), curcuminoids (120 mg/9cm^2), diosgenin (20 mg/9cm^2) and rutin (125mg/9cm^2) were accurately weighed, dissolved in ethanol and added to polymeric dispersion. The solution was casted on the backing membrane placed in a petridish and dried at room temperature for 24 hrs. An inverted funnel was placed over the petridish to prevent fast evaporation of the solvent. After 24 hrs the dried patches were taken out, cut into small pieces (9 cm^2) and stored in desiccators for further studies (Patel et al., 2009).

Optimization of patch by Full Factorial design

A 2^3 full factorial design was applied for optimization of variables like, concentration of Eudragit RL 100, concentration of Eudragit RS 100 and %w/w of menthol. Tensile strength and Q_{24} (% drug release at 24 hrs) were taken as dependent variables in this study. Multiple linear regression analysis, Analysis of Variance (ANOVA) and graphical representation of the influence of factors by contour plots and 3D surface plots were performed using Minitab software. The formulation layout for the factorial design batches is shown in Table 1. (Rao et al., 2019)

Table 1: Design layout for 2^3 full factorial batches of transdermal patch

Formulation code	Coded value			Uncoded value		
	Concentration of Eudragit RL 100 (X1)	Concentration of Eudragit RS 100 (X2)	% w/w of menthol (X3)	Concentration of Eudragit RL 100 (X1) (mg)	Concentration of Eudragit RS 100 (X2) (mg)	% w/w of menthol (X3)
P1	−1	+1	−1	200	800	3
P2	−1	+1	+1	200	800	5
P3	−1	−1	−1	200	200	3
P4	−1	−1	+1	200	200	5
P5	+1	+1	−1	800	800	3
P6	+1	+1	+1	800	800	5
P7	+1	−1	−1	800	200	3
P8	+1	−1	+1	800	200	5

Physicochemical evaluation

All factorial design batches were evaluated for following parameters (Prabhakar, et al., 2013).

Thickness of patch

The thickness of the drug loaded transdermal patch was measured at three different places using a micrometer. Mean values and standard deviations were calculated for the data.

Weight of patch

A specified area (9 cm^2) of dried patch was cut in different parts of the patch and weighed on digital balance. The average weight and standard deviation values were calculated from the individual weights.

Percentage Flatness

A transdermal patch should possess a smooth surface and should not constrict with time.
This can be demonstrated with flatness study. Three longitudinal strips were cut out from each film:1 from the center, 1 from the left side, and 1 from the right side. The length of each strip was measured and the variation in length because of non-uniformity in flatness was measured by determining percent constriction, with 0% constriction equivalent to 100% flatness.

Folding endurance

Evaluation of folding endurance involves determining the folding capacity of the films subjected to frequent extreme conditions of folding. This was determined by repeatedly folding one film at the same place till it broke. The number of times the film could be folded at the same place without breaking/cracking gave the value of folding endurance.

Tensile strength

To determine the elongation as a tensile strength, the polymeric patch was pulled by means of a pulley system; weights were gradually added to the pan to increase the pulling force till the patch was broken. The weight needed to break the patch was noted and the tensile strength was calculated as kg/cm^2.

Percentage Moisture content

The films were weighed individually and kept in a desiccator containing activated silica at room temperature for 24 hours. Individual films were weighed repeatedly until they showed a constant weight. The films were reweighed and percentage of moisture content was calculated as the difference between initial and final weight with respect to final weight.

Percentage Moisture uptake

The films were weighed individually and kept in a desiccator containing saturated solution of potassium chloride to maintain 84% RH for 24 hours. The films were reweighed and percentage of moisture uptake was calculated as the difference between final and initial weight with respect to initial weight.

Water vapour transmission rate (WVTR)

WVTR is defined as the quantity of moisture transmitted through unit area of film in unit time. Glass cells were filled with 2 g of anhydrous calcium chloride and a film of specified area was affixed onto the cell rim. The assembly was accurately weighed and placed in a humidity chamber (80 $\pm$ 5% RH) at 27 $\pm$ 2 °C for 24 hours. Then the cells were reweighed and WVTR was determined by following formula.

WVTR = Final weight – initial weight Area $\times$ 24

Drug content

A specified area of patch (1 cm^2) was dissolved in 100 ml methanol and kept in the ultrasonicator for 20 min. The solutions were filtered through a 0.45 µm membrane, diluted suitably and analyzed for the content of each drug by the developed HPTLC methods.

In-vitro drug release study

In-vitro drug release study was performed using a Franz Diffusion Cell (FDC) with a receptor compartment capacity of 20 ml. A cellophane membrane was used for the determination of drug release from the prepared transdermal matrix type patches. The receptor compartment of the diffusion cell was filled with phosphate buffer pH 5.5 containing 1% Tween 80. The sample was withdrawn at predetermined time up to 24 hrs and analyzed for drug content by HPTLC method (Prabhakar, et al., 2013).

Ex-vivo skin permeation study of optimized patch

An ex-vivo permeation study was carried out on selected batch using Franz diffusion cell. Abdominal skin of male Wistar rat (230 to 250 gm body weight) was used. The sample was withdrawn at predetermined time up to 24 hrs and analyzed for drug content by HPTLC method. The cumulative amount of drugs permeated per unit area was plotted against time and the slope of the linear portion of the plot was estimated as steady-state flux (Jss) and the lag time was determined by extrapolating the linear portion of the curve to the abscissa. The permeability coefficient (Kp) was calculated by using the equation Kp = Jss/Cv, where Cv is the total concentration of drug in the patch (Rao et al., 2019).

Kinetic modeling of skin permeation data

The ex-vivo skin permeation data were fitted to various kinetic models such as zero order, first order, Higuchi, Korsemeyer and Peppas to ascertain the kinetic of drug release. The method described by Korsemeyer and Peppas was used to describe mechanism of drug release (Patel et al., 2009).

Accelerated stability study

The optimized batch was packed in aluminium foil and kept at 40^0C-75% Relative Humidity (RH) for 90 days. After 90 days, patches were analyzed for physical appearance, drug content and in-vitro release profile (Patel et al., 2009).

Primary skin irritation study of formulated polyherbal transdermal patch

Animals

Wistar albino rats (body weight: 200-250g) were used for the skin irritation study. They were kept in standard experimental conditions viz. housing in standard polypropylene cages on a 12hrs light-dark cycle. The rats were fasted for 12hrs before commencement of study but allowed access to water. All the animals were maintained in accordance with guidelines of Committee for the Purpose of Control and Supervision of Experiments on Animals (CPCSEA).

Treatment protocol

The animal study protocol (BKMGPC/IAEC19/RP29/2017) was approved by Institutional Animal Ethics Committee (IAEC) under CPCSEA guidelines. Animals were divided into four groups (n=6 in each group) as shown in Table 2.

Table 2: Groups and treatments for skin irritation study

Group	No. of animals	Group name	Formulation/Treatment
I	6	Normal control	Adhesive tap USP
II	6	Standard irritant	0.8% v/v aqueous formalin solution
III	6	Polymeric patch	Non medicated patch
IV	6	Test patch	Formulated medicated patch

On the previous day of the experiment, the hair on the dorsal area of rats was removed. Prepared polyherbal patch was applied on shaved area by means of adhesive tap USP. Dermal responses were observed and scored after 24 hr exposure and thereafter at 48 hr, 72 hr and at 7 days after patch removal. The skin reactions, defined as erythema or edema were evaluated according to the scoring system for skin reactions (Table 3) as reported by Draize et al. (1994). Scores are assigned from 0 to 4 based on the severity of erythema or edema formation. The Score of Primary Irritation (SPI) was calculated for each rat as the following.

SPI for each rat = Σ Erythema and edema grade on each day
No. of observations

Table 3: Classification system for skin reactions

Skin responses	Score
Erythema and Eschar formation	
No Erythema	0
Very slight Erythema	1
Well defined Erythema	2
Moderate to severe Erythema	3
Severe Erythema	4
Edema formation	
No Edema	0
Very slight Edema	1
Slight Edema	2
Moderate Edema	3
Severe Edema	4
Total possible score for irritation	**8**

The difference between the summation of SPI scores of six animals from the treated site and control site were calculated and were used for Primary Irritation Index (PII) determination. PII was calculated as the arithmetical mean of the SPI values of the six rats. The irritation degree was categorized as negligible or slight, moderate or severe irritation based on the PII as shown in Table 4.

PII = Σ SPI (Test) – Σ SPI (Control)
No. of animals

Table 4: Response categories of irritations in rats

Category	Primary Irritation Index (PII)
Negligible	0–0.4
Slight irritation	0.5–1.9
Moderate	2–4.9
Severe	5–8

Result and Discussion

Authentication of plant materials

Plant materials were authenticated by comparing their morphological and microscopical characters with those reported in the literature (GoI 1999 a, b RRL 1998).

Oleogum resin of Boswellia serrata

Oleogum resin of Boswellia serrata contained stalactic, transparent tears of roundish, club shaped, pear shape and irregular shaped and various sizes. It is brownish yellow, up to 5 cm long, 2 cm thick, fragrant, fracture brittle; fractured surface waxy and translucent; burned readily and emanated an agreeable characteristic, balsamic resinous odour; taste, aromatic and agreeable. These macroscopic characters were comparable with those mentioned for oleogum resin of Boswellia serrata in literature (GoI 1999a).

Turmeric powder

Turmeric powder was fine, yellowish powder. It had aromatic odour and taste. Microscopical studies showed presence of following characters in turmeric powder as shown in Fig. 2. a) Annular and spiral xylem vessels, b) Cork in surface view, c) Large spherical cortical parenchymatous cells containing dense coloring pigment, starch grains and oleoresin cells were scattered in the powder, d) Fragments of reticulate vessels, e) Simple starch grains. These morphological and microscopic characters were comparable with those mentioned for turmeric powder in literature (GoI 1999b, RRL 1998).

Isolation and characterization of phytochemicals

Boswellic acids

Boswellic acids consisted of a mixture of 4 boswellic acid derivatives, namely β-boswellic acid, 3-acetyl β-boswellic acid, 11-keto β-boswellic acid and 3-acetyl 11-keto β-boswellic acid. Isolated boswellic acids mixture was creamy white colored powder and yield was 12 %w/w. It was used as such because all the components of boswellic acids are reported to have anti-inflammatory activity. Hence, further purification to the level of individual compounds would not give any added advantage over the crude mixture form. The IR spectral analysis showed that the principal peaks were observed at wavenumber 3485, 2924, 1707, 1448 and 1240 cm^{-1}, confirming the purity of the drug (Fartyal et al., 2011). (Mohan et al., 2012).

Curcuminoids

Curcuminoids contained a mixture of curcumin, demethoxycurcumin and bisdemethoxycurcumin. All the components are reported to have anti-inflammatory activity. Hence, further purification is not required. Isolated curcuminoids was in the form of orange colored crystalline powder and yield was 27%w/w. The IR spectral analysis showed that the principal peaks were observed at wavenumber 3504, 2943, 1710, 1625, 1274 and 960 cm^{-1}, confirming the purity of the drug (Mohan et al., 2012).

Diosgenin

Diosgenin was obtained as white powder. Its melting point was found to be 208 + 0.65 °C. The IR spectral analysis showed that the principle peaks were observed at wavenumber 3446, 2949, 1710, 1452, 1371 and 1051 cm^{-1}, confirming the purity of the drug (Indrayanto et al., 1994).

Rutin

Rutin was obtained as yellow powder. Its melting point was found to be 242 + 0.55 °C. The IR spectral analysis showed that the principle peaks were observed at wavenumber 3327, 2304, 1710, 1597, 1361 and 1060 cm^{-1}, confirming the purity of the drug (Panhwar et al., 2014).

Development of HPTLC methods for analysis of phytochemicals

HPTLC methods were developed for the analysis of the phytochemicals in the patch. Since diosgenin and boswellic acids do not have UV chromophore, their analysis by HPLC would require special detectors like refractive index detector or evaporative light scattering detector. HPTLC is suitable for analysis of such compounds because it allows for post-chromatographic derivatization, which renders such compounds detectable in UV-visible spectrum.

HPTLC method was developed for all phytochemicals in two different mediums. One medium is methanol solvent which was used for the estimation of drug content. Another medium was diffusion medium, PBS of pH 5.5 containing 1% Tween 80, which was used for analysis of these compounds during the drug release study and skin permeation study.

Calibration curve of Phytochemicals in methanol

The mobile phase, n-hexane: acetone (7:3), gave good resolution with Rf 0.54 for boswellic acids, 0.30 for curcuminoids and 0.62 for diosgenin in methanol. The mobile phase, ethyl acetate: glacial acetic acid: formic acid: water (100:11:11:25), gave good resolution with Rf 0.48 for rutin. Under the chromatographic condition employed, standard compound, rutin exhibited sharp peaks and good resolution (Figure 2 - 3).

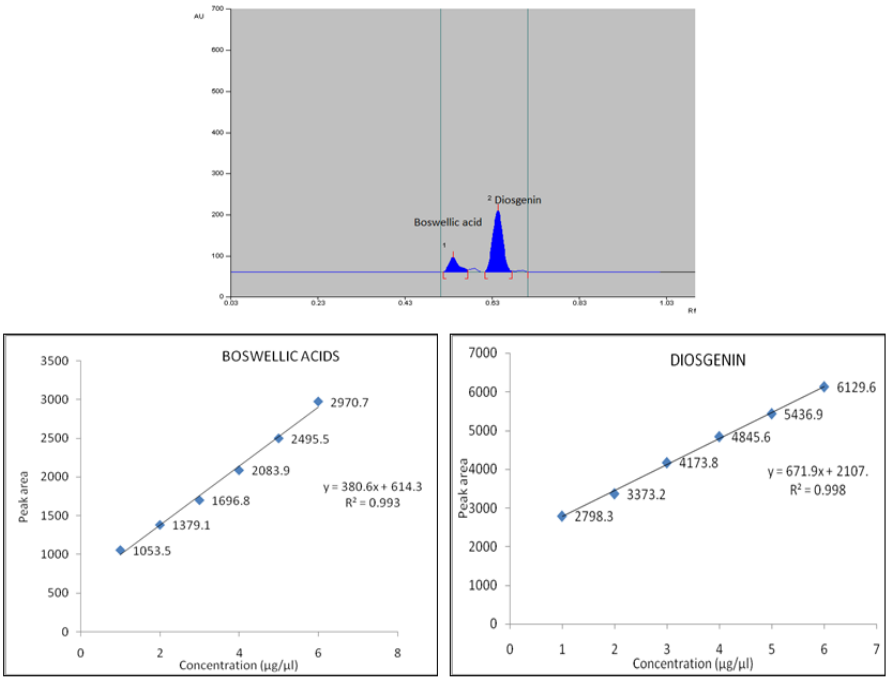

Figure 2: HPTLC chromatogram and calibration curve of standard boswellic acids and diosgenin in methanol

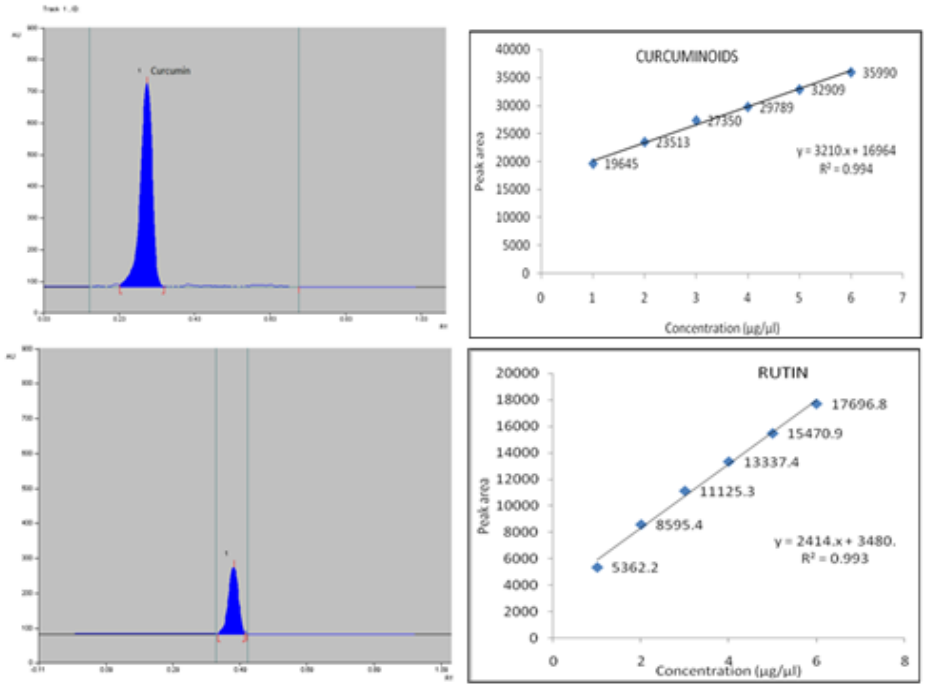

Figure 3: HPTLC chromatogram and calibration curve of standard curcuminoids and rutin in methanol

Calibration curve of Phytochemicals in diffusion medium

The mobile phase, n-hexane: acetone (7:3), gave good resolution with Rf 0.57 for boswellic acids, 0.42 for curcuminoids and 0.93 for diosgenin in diffusion medium. The mobile phase, ethyl acetate: glacial acetic acid: formic acid: water (100:11:11:25), gave good resolution with Rf 0.48 for rutin. Under the chromatographic condition employed, standard phytochemicals exhibited sharp peaks and good resolution (Figure 4).

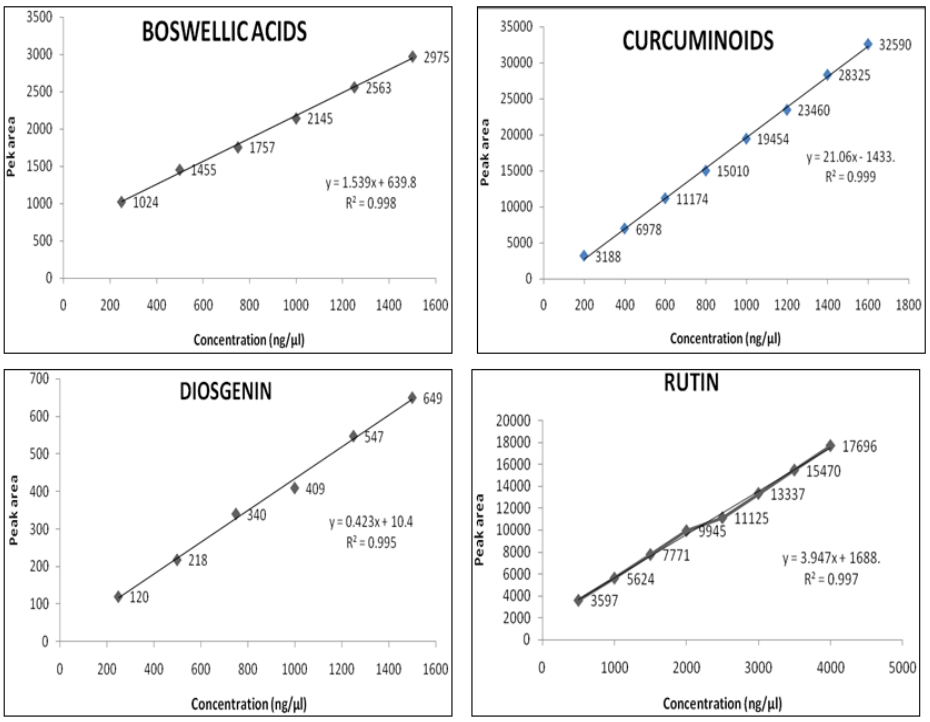

Figure 4: Calibration curve of standard boswellic acid, curcuminoids, diosgenin and rutin in diffusion medium by HPTLC

The linearity ranges of these compounds obtained by the developed HPTLC methods were sufficient to quantify these compounds from the dissolution medium during drug-release study and skin-permeation study.

Selection of excipients

Selection of polymers

All the trial batches were almost similar as far as % flatness was concerned. However, patch made up of Eudragit RL 100 and Eudragit RS 100 exhibited maximum folding endurance. Moreover, the density of said patch was the highest among all batches. Hence batch containing Eudragit RL 100 and Eudragit RS 100 as polymers was found to have desirable properties. Eudragit RL 100 is relatively more permeable to water than Eudragit RS 100. An optimum combination of the Eudragit RL 100 and Eudragit RS 100 could be able to achieve desired release profile. So other batches were eliminated and concentration of Eudragit RL 100 and Eudragit RS 100 were assigned as independent variable in 2^3 factorial designs to understand their effect and to optimize concentration of both for desired release profile.

Selection of plasticizers

As all the drugs are lipophilic in nature, hydrophilic plasticizer was preferred. Polyethylene glycol 400 was selected as a plasticizer as it showed maximum folding endurance and is hydrophilic in nature.

Selection of backing membrane

Among the five trial batches of transdermal patches prepared for selection of backing membrane, the one prepared using 5% polyvinyl alcohol (PVA) exhibited low WVTR and sufficient tensile strength. Increasing the concentration of PVA beyond 5% did not lead to significant change in WVTR and tensile strength. Hence 5% PVA was selected as a backing membrane for all further batches of transdermal patches.

Selection of permeation enhancers

Penetration enhancers from natural origin offer several benefits over synthetic and chemical permeation enhancers, such as sustainable mass production from a renewable resource and lower cost depending on the type of extraction used. Menthol, a monocyclic monoterpene free from toxic effects, has been approved as a penetration enhancer in the transdermal delivery of several drugs. So, menthol was selected as a permeation enhancer. The concentration of menthol was optimized by full factorial design.

Drug excipients compatibility studies by FTIR and DSC

FTIR Study

Drug-excipients interactions play a vital role in the release of drug from formulation. FTIR spectroscopic analysis of drug mixture and its combination with polymers was performed to study the physical and chemical interactions between them. It was observed that there were no or very minor changes in IR spectra of drug mixture alone and/ after mixing with polymers. The FTIR study revealed no physical or chemical interactions of drugs with Eudragit RL 100 and Eudragit RS 100 as shown in Table 5.

Table 5: FTIR study of drugs and excipients

Wave numbers of Drug mixture (cm^{-1})	Wave numbers of Drug mixture + Eudragit RL 100 + Eudragit RS 100 (cm^{-1})	Inference
2920, 1627, 1600, 1457, 1500, 1428, 1366, 1274, 1233, 1205, 1179, 1054, 1025	2952, 1627, 1600, 1451, 1377, 1235, 1144, 1067, 963	Drugs and polymers are compatible.

DSC Study

The DSC thermograms of drug mixture, polymers and mixture of drugs with polymers were recorded. The thermogram showed sharp distinct endothermic peak for each drug in drug mixture. The endothermic peaks corresponding to the drugs were also present in the thermograms of drug polymer mixtures (Table 6). This suggests that there is no significant interaction between the drugs and the polymers.

Table 6: Compatibility studies of drug and polymer by DSC thermograms

Drug/drug-polymer combination	Observed Peaks (^0C)
Drug mixture	226.38, 179.27, 207.47, 247.49
Eudragit RL 100 + Eudragit RS 100	260.92, 59.16
Drug mixture + Eudragit RL 100 + Eudragit RS 100	230.31, 175.55, 205.11, 252.36, 262.58

Full Factorial design for optimization of formulation variables

A 2^3 full factorial design was used to optimize the variables for formulation of transdermal patch. An optimized combination of Eudragit RL 100 and Eudragit RS 100 may be able to achieve desired drug release. Hence amount Eudragit RL 100, amount of Eudragit RS 100 and amount of menthol were assumed as independent variables in a 2^3 full factorial design. The tensile strength and Q_{24} (% cumulative drug release at 24 hrs) were taken as dependent variables. The results are presented in Table 7.

Table 7: Experimental runs and measured responses of 2^3 full factorial design batches of transdermal patch

Formulation code	Tensile strength* (Kg/cm^2)	Q_{24} (% Drug release at 24 hr)			
		Boswellic acids	Curcuminoids	Diosgenin	Rutin
P1	3.43 ± 0.058	14.51	78.62	7.5	72.05
P2	3.40 ± 0.100	16.37	79.00	8.86	74.04
P3	2.37 ± 0.115	10.54	73.68	6.83	64.11
P4	2.10 ± 0.100	12.27	76.07	7.5	66.86
P5	2.87 ± 0.058	21.84	80.01	9.54	74.86
P6	2.70 ± 0.100	23.75	82.68	10.22	76.64
P7	1.77 ± 0.153	24.43	83.03	10.9	78.02
P8	1.57 ± 0.058	27.91	86.64	11.57	80.77

*Values are expressed as Mean ± SD (n = 3)

The formulation P8 had maximum release of all four drugs after 24 hr. However, the tensile strength of P8 batch was the least of all other factorial design batches. Based on Q_{24} values, batch P8 was selected as optimized batch. Though the tensile strength was low, it was not below the desirable limit.

Physicochemical evaluation of factorial design batches

The factorial design batches were evaluated for thickness, weight of patch, % flatness, folding endurance, % moisture content, % moisture uptake, WVTR and drug content study. The results are presented in Table 8 and Table 9.

Table 8: Result of evaluation parameters of 2^3 full factorial design batches of transdermal patch

Formulation code	Thickness* (mm)	Weight * (g/9cm²)	% Flatness*	Folding endurance*
P1	0.36+0.02	0.293+0.0180	99.47+0.280	70.33+2.52
P2	0.38+0.02	0.3+0.0196	99.60+ 0.156	74.00+4.58
P3	0.25+0.03	0.168+0.0195	99.64+ 0.439	57.00+3.61
P4	0.24+0.02	0.218+0.02	99.52+ 0.189	53.00+2.65
P5	0.55+0.04	0.470+0.0135	99.52+ 0.421	65.67+2.08
P6	0.57+0.03	0.402+0.0091	99.67+ 0.211	57.67+1.53
P7	0.41+0.03	0.346+0.0345	99.52+ 0.434	76.00+3.61
P8	0.42+0.02	0.373+0.0285	99.56+ 0.269	79.33+1.73

*Values are expressed as Mean ± SD (n = 3)

Table 9: Result of evaluation parameters of 2^3 full factorial design batches of transdermal patch

Formulation code	% Moisture content*	% Moisture uptake*	WVTR* (g/cm²24hr)	Drug content (%w/w)			
				Boswellic acids	Curcuminoids	Diosgenin	Rutin
P1	1.37 ± 0.09	2.22 ±0.07	2.48 ±0.15	98.89	98.85	98.85	99.95
P2	1.70 ±0.09	2.43 ±0.22	2.89 ±0.06	99.12	99.47	98.12	99.31
P3	2.18 ±0.17	2.52 ±0.18	3.19 ±0.23	98.36	100.34	99.23	98.32
P4	2.44 ±0.06	2.82 ±0.05	3.39 ±0.14	99.37	100.12	99.18	98.79
P5	2.69 ±0.06	3.16 ±0.20	3.67 ±0.12	100.84	99.63	100.75	99.78
P6	2.74 ±0.31	3.44 ±0.16	3.96 ±0.21	100.98	100.29	100.81	100.02
P7	3.37 ±0.18	3.70 ±0.08	4.09 ±0.15	99.42	99.64	99.52	100.48
P8	3.84 ±0.06	4.10 ±0.15	4.48 ±0.18	99.74	99.84	99.12	99.43

*Values are expressed as Mean ± SD (n = 3)

Among P1 to P8 formulations, P8 showed lowest tensile strength, highest % moisture content, % moisture uptake, WVTR and folding endurance. Increase in the tensile strength of patch was observed with an increase in the concentration of Eudragit RS 100 in the patch. However, Eudragit RL 100 and menthol had a negative influence on tensile strength.

In-vitro drug release study

In-vitro drug release data of 2^3 full factorial design batches of transdermal patch for each drug are shown in Figure 5.

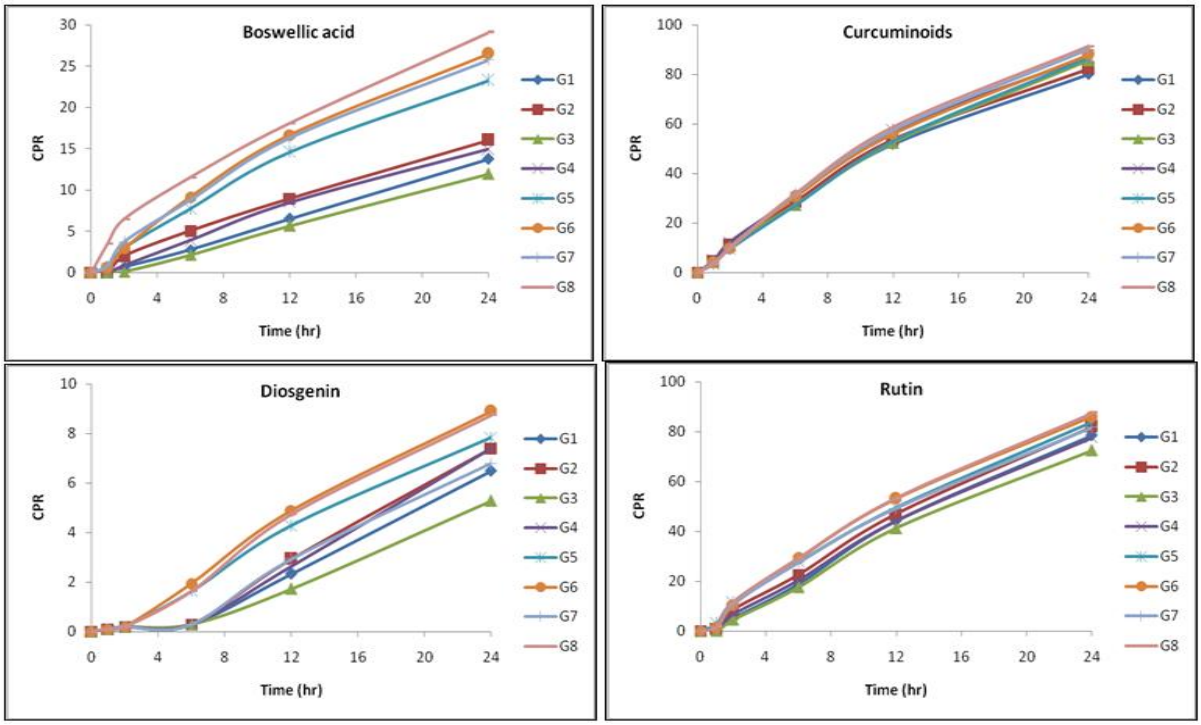

Figure 5: Cumulative percentage release of boswellic acids, curcuminoids, diosgenin and rutin from factorial design batches of transdermal patch

The formulation P5-P8 had shown high % release of drugs compared to formulation P1-P4. This may be due to high % of hydrophilic polymer, Eudragit RL 100. From the graph of cumulative % drug release vs. time, it can be concluded that the drug release appeared to increase more with an increasing amount of the Eudragit RL 100 as compared to Eudragit RS 100. Eudragit RL 100 is freely permeable to water whereas Eudragit RS 100 is slightly permeable to water. Eudragit RL 100 possesses more ammonium content as compared to the Eudragit RS 100. Eudragit RS 100, because of its hydrophobic nature, might slow down the release of drug from the patch. A marked effect of menthol on release of drugs was observed.

Optimization of transdermal patch by 2^3 Full Factorial Design

A statistical model incorporating interactive and polynomial terms was used to evaluate the responses.

$Y=b_0 + b_1X_1 + b_2X_2 + b_3X_3 + b_{12} X_1X_2 + b_{13} X_1X_3 + b_{23} X_2X_3 + b_{123}X_1X_2X_3$

where Y is the dependent variable, b_0 is the arithmetic mean response of the 8 runs and any bi is the estimated coefficients for the related factor Xi. The main effects (X_1, X_2 and X_3) represent the average result of changing one factor at a time from its low to high value. The interaction term (X_1X_2, X_1X_3, X_2X_3, $X_1X_2X_3$) shows how the response changes when the two factors change simultaneously. The fitted equations (full model) relate the responses that are, tensile strength and Q_{24} (% drug release at 24 hrs), to the transformed factor. The polynomial equations can be used to draw conclusions after considering the magnitude of coefficient and the mathematical sign it carries (i.e. positive or negative).

The results of ANOVA suggested that F values calculated for tensile strength, Q_{24} of boswellic acids, Q_{24} of curcuminoids, Q_{24} of diosgenin and Q_{24} of rutin are 1108.492, 8335.282, 2294.705, 1526.026 and 2624.037, respectively (Table 10).

Table 10: Results of the ANOVA for dependent variables

Source of variation	DF	SS	MS	F	P
Tensile strength					
Regression	7	4.310802	0.615829	1108.492	0.02312
Residual	1	0.000556	0.000556		
Total	8	4.311358			
Q_{24} of Boswellic acids					
Regression	7	352.9992	50.42845	8335.282	0.0084
Residual	1	0.00605	0.00605		
Total	8	353.0052			
Q_{24} of curcuminoids					
Regression	7	157.4168	22.48811	2294.705	0.016
Residual	1	0.0098	0.0098		
Total	8	157.4266			
Q_{24} of Diosgenin					
Regression	7	26.17135	3.738764	1526.026	0.0197
Residual	1	0.00245	0.00245		
Total	8	26.1738			
Q_{24} of Rutin					
Regression	7	265.4214	37.91734	2624.037	0.015
Residual	1	0.01445	0.01445		
Total	8	265.4358			

Tabulated F value was found to be 236.76 at $\alpha = 0.05$. Calculated F values are greater than tabulated F value. Therefore, all selected factors have shown significant effects. R^2 value for tensile strength, Q_{24} of boswellic acids, Q_{24} of curcuminoids, Q_{24} of diosgenin and Q_{24} of rutin are 0.9998, 0.9991, 0.9938, 0.9906 and 0.9946 respectively, indicating good correlation between dependent and independent variables.

The reduced models were developed for response variables by omitting the insignificant terms with $P > 0.05$. The terms with $P < 0.05$ were considered statistically significance and retained in the reduced model. The coefficients for full model (Fm) and reduced model (Rm) for response variables are shown in Table 11.

Table 11: Summary of regression output of significance factors

Responses	Model	Coefficient of regression parameters								
		b0	b1	b2	b3	b12	b13	b23	b123	R^2
Tensile strength	Fm	2.522	-0.302	0.577	-0.0854	-0.015	-0.0104	0.0354	-0.0229	0.9998
	Rm	2.522	-0.303	0.577	-0.0861					0.9959
CPR of Boswellic acids	Fm	18.946	5.523	0.171	1.115	-1.846	0.218	-0.173	-0.205	0.9991
	Rm	19.149	5.726	-0.032	1.319					0.9088
CPR of curcuminoids	Fm	79.98	3.137	0.142	1.145	-1.825	0.452	-0.337	0.165	0.9938
	Rm	80.184	3.341	-0.062	1.349					0.7876
CPR of Diosgenin	Fm	9.110	1.438	-0.081	0.418	-0.588	-0.0894	0.0918	-0.0806	0.9906
	Rm	9.151	1.478	-0.121	0.458					0.8811
CPR of Rutin	Fm	73.40	4.143	0.989	1.148	-	-	-	-	0.994

		8				2.791	0.0369	0.205	0.0156	6
	Rm	73.656	4.391	0.741	1.396					0.7416

Full and Reduced Model for Tensile Strength

For Tensile strength, as seen from Contour plots and 3D surface plots (Figure 6) revealed that a corresponding increase in the Tensile strength of patch was observed with increase in concentrations of Eudragit RS 100. From the graphs and the regression coefficient values of all factors it can be concluded that increase in tensile strength is more with an increasing amount of the Eudragit RS 100 as compared to Eudragit RL 100 and menthol.

For Tensile strength, the significance levels of the coefficients b12, b13, b23 and b123 were found to be P =0.321, 0.419, 0.142 and 0.215 respectively, so they were omitted from the full model to generate a reduced model. The coefficients b1, b2 and b3 were found to be significant at $P < 0.05$; hence they were retained in the reduced model. The reduced model for Tensile strength,

TS = 2.522 + (−0.303 * X1) + (0.577 * X2) + (−0.0861*X3)

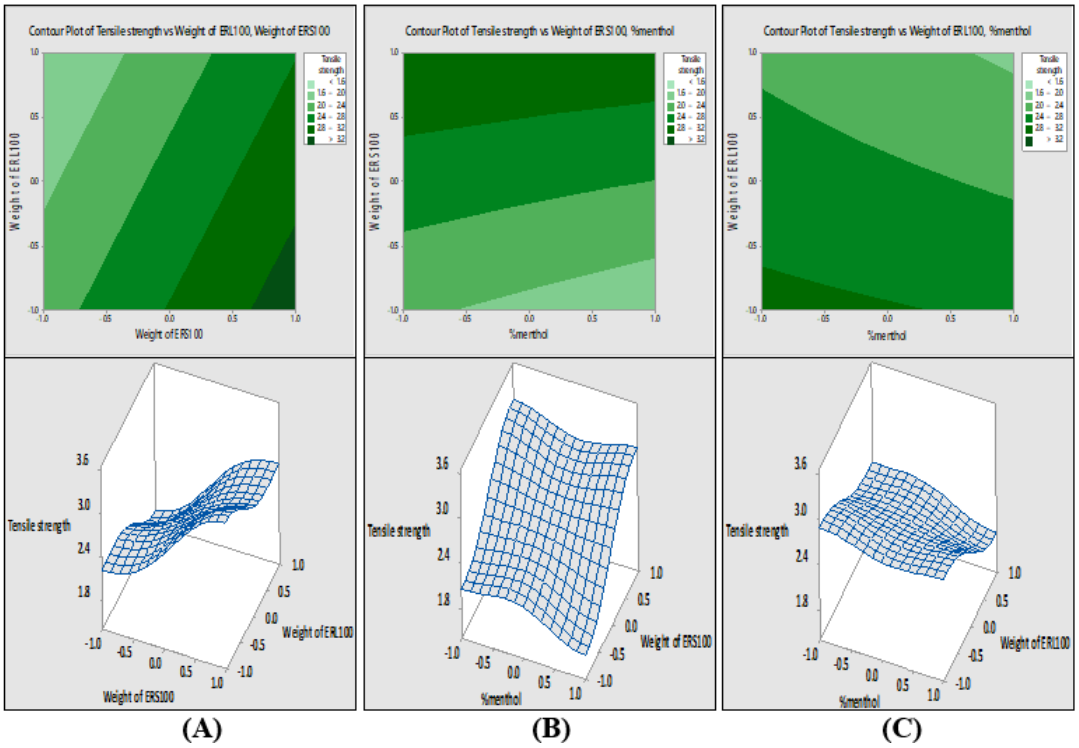

Figure 6: Response surface plot for tensile strength

(A) Effect of weight of ERL 100 (mg) X1 and weight of ERS 100 (mg) X2 on response Y1 (Tensile strength) (B) Effect of weight of ERS 100 (mg) X2 and concentration of Menthol (%w/w) X3 on response Y1 (Tensile strength) (C) Effect of weight of ERL 100 (mg) X1 and concentration of Menthol (%w/w) X3 on response Y1 (Tensile strength).

Full and Reduced Model for Q_{24} of Boswellic acids

A corresponding decrease in the % boswellic acids release of patch was observed with increase in concentrations of Eudragit RS 100. From the Contour plots, 3D surface plots (Figure 7) and the regression coefficient values of all factors, it can be concluded that the boswellic acids release appeared to decrease more with an increasing amount of the Eudragit RS 100 as compared to Eudragit RL 100 and menthol. The more decrease in the drug release by Eudragit RS 100 as

compared to Eudragit RL 100 could be explained by difference in the permeability characteristics. Eudragit RL 100 is freely permeable to water whereas Eudragit RS 100 is slightly permeable to water. Eudragit RL 100 possesses more ammonium content as compared to the Eudragit RS 100.

For Q_{24} of Boswellic acids, the significance levels of the coefficients b12, b13, b23 and b123 were found to be P = 0.009, 0.07, 0.09 and 0.08 respectively, so they were omitted from the full model to generate a reduced model. The coefficients b1, b2 and b3 were found to be significant at $P < 0.05$; hence they were retained in the reduced model. The reduced model for Q_{24} of Boswellic acids,

$Q_{24} = 19.149 + (5.726* X1) + (-0.032* X2) + (1.319*X3)$

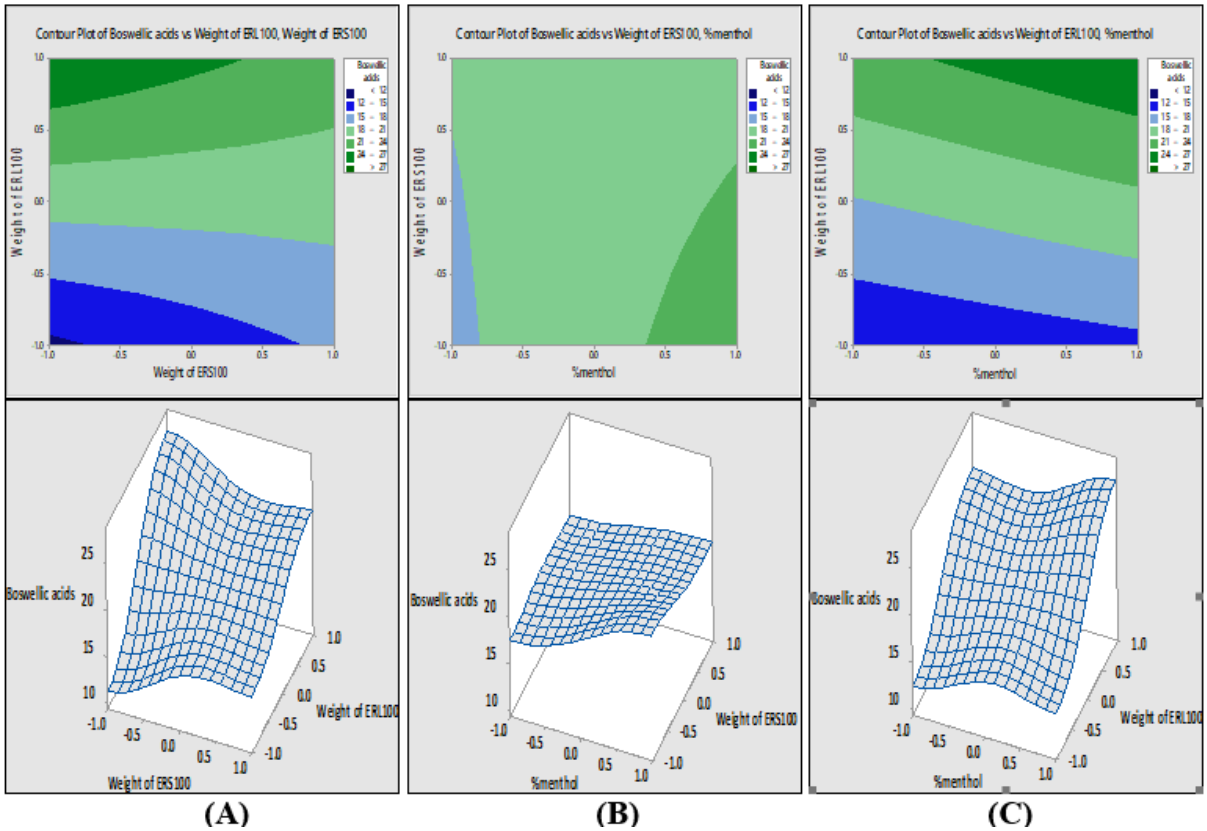

Figure 7: Response surface plot for Q24 of boswellic acids

(A) Effect of weight of ERL 100 (mg) X1 and weight of ERS 100 (mg) X2 on response Y2 (Q24 of boswellic acids) (B) Effect of weight of ERS 100 (mg) X2 and concentration of Menthol (%w/w) X3 on response Y2 (Q24 of boswellic acids) (C) Effect of weight of ERL 100 (mg) X1 and concentration of Menthol (%w/w) X3 on response Y2 (Q24 of boswellic acids)

Full and Reduced Model for Q_{24} of Curcuminoids

A corresponding decrease in the % Curcuminoids release of patch was observed with increase in concentrations of Eudragit RS 100. From the Contour plots, 3D surface plots (Figure 8) and the regression coefficient values of all factors, it can be concluded that the Curcuminoids release appeared to decrease more with an increasing amount of the Eudragit RS 100 as compared to Eudragit RL 100 and menthol. The more decrease in the drug release by Eudragit RS 100 as compared to Eudragit RL 100 could be explained by difference in the permeability characteristics. Eudragit RL 100 is freely permeable to water whereas Eudragit RS 100 is slightly permeable to water. Eudragit RL 100 possesses more ammonium content as compared to the Eudragit RS 100.

For Q_{24} of Curcuminoids, the significance levels of the coefficients b12, b13, b23 and b123 were found to be P = 0.0118, 0.0475, 0.063 and 0.128 respectively, so they were omitted from the full model to generate a reduced model. The coefficients b1, b2 and b3 were found to be significant at $P < 0.05$; hence they were retained in the reduced model. The reduced model for Q_{24} of Curcuminoids,

$Q_{24} = 80.184 + (3.341* X1) + (-0.062* X2) + (1.349*X3)$

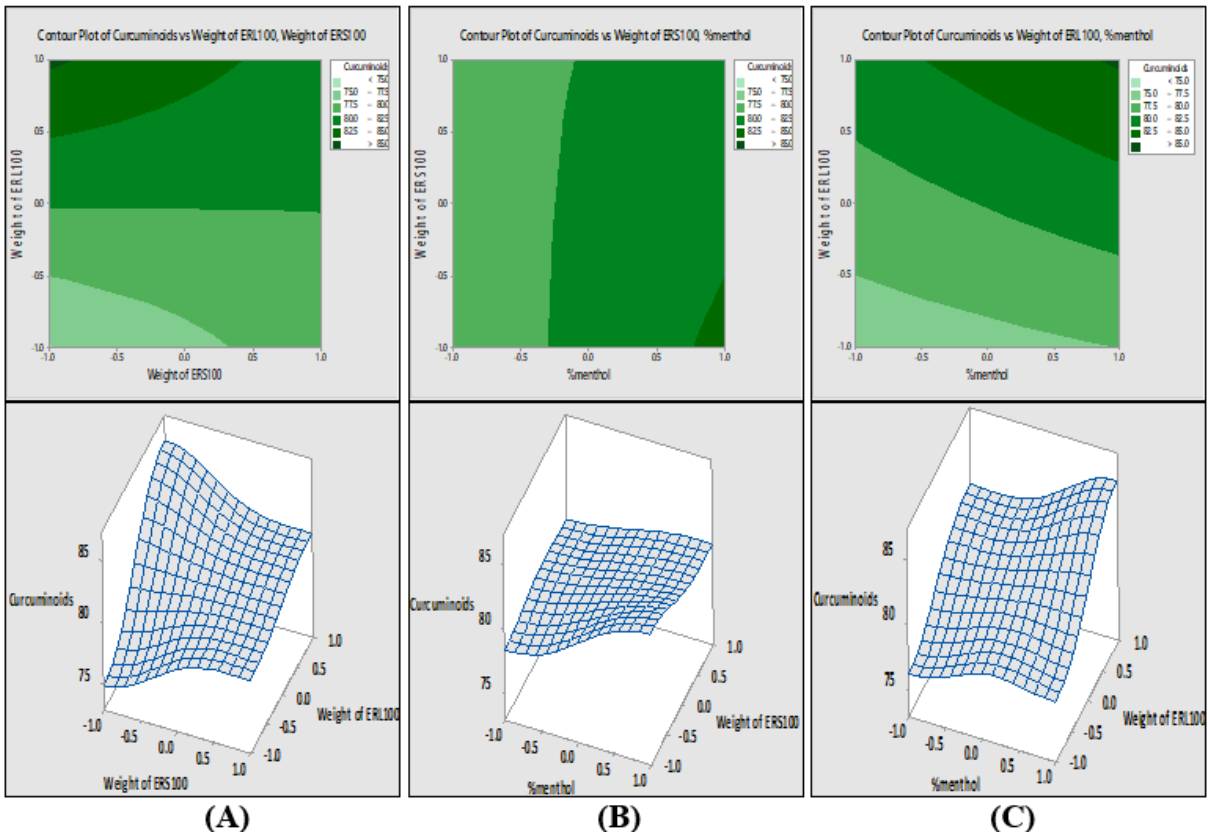

Figure 8: Response surface plot for Q24 of curcuminoids

(A) Effect of weight of ERL 100 (mg) X1 and weight of ERS 100 (mg) X2 on response Y2 (Q24 of curcuminoids) (B) Effect of weight of ERS 100 (mg) X2 and concentration of Menthol (%w/w) X3 on response Y2 (Q24 of curcuminoids) (C) Effect of weight of ERL 100 (mg) X1 and concentration of Menthol (%w/w) X3 on response Y2 (Q24 of curcuminoids)

Full and Reduced Model for Q_{24} of Diosgenin

A corresponding decrease in the % Diosgenin release of patch was observed with increase in concentrations of Eudragit RS 100. From the Contour plots, 3D surface plots (Figure 9) and the regression coefficient values of all factors, it can be concluded that the Diosgenin release appeared to decrease more with an increasing amount of the Eudragit RS 100 as compared to Eudragit RL 100 and menthol. The more decrease in the drug release by Eudragit RS 100 as compared to Eudragit RL 100 could be explained by difference in the permeability characteristics. Eudragit RL 100 is freely permeable to water whereas Eudragit RS 100 is slightly permeable to water. Eudragit RL 100 possesses more ammonium content as compared to the Eudragit RS 100.

For Q_{24} of Diosgenin, the significance levels of the coefficients b12, b13, b23 and b123 were found to be P = 0.0183, 0.1192, 0.1161 and 0.1318 respectively, so they were omitted from the full model to generate a reduced model. The coefficients b1, b2 and b3 were found to be

significant at $P < 0.05$; hence they were retained in the reduced model. The reduced model for Q_{24} of Diosgenin,

$Q_{24} = 9.151 + (1.478^* X1) + (-0.121^* X2) + (0.458^*X3)$

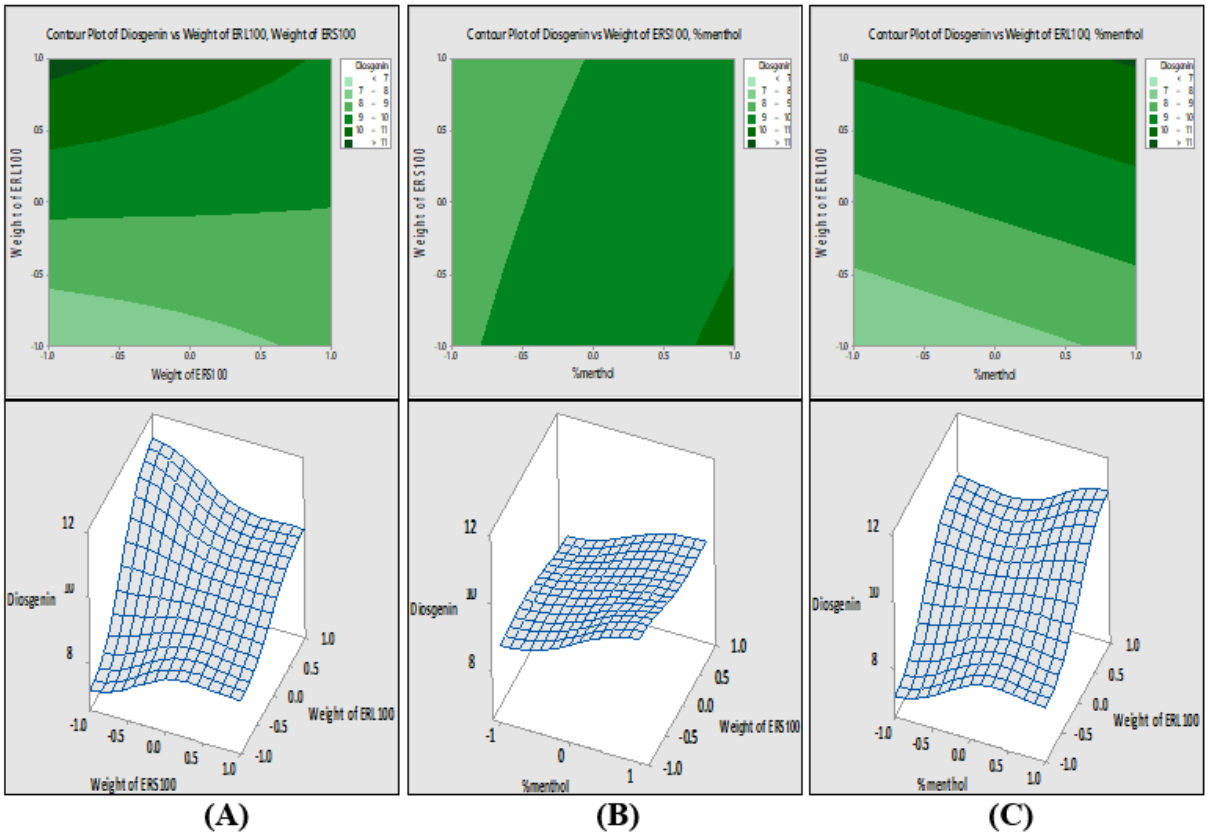

Figure 9: Response surface plot for Q24 of diosgenin

(A) Effect of weight of ERL 100 (mg) X1 and weight of ERS 100 (mg) X2 on response Y2 (Q24 of diosgenin) (B) Effect of weight of ERS 100 (mg) X2 and concentration of Menthol (%w/w) X3 on response Y2 (Q24 of diosgenin) (C) Effect of weight of ERL 100 (mg) X1 and concentration of Menthol (%w/w) X3 on response Y2 (Q24 of diosgenin)

Full and Reduced Model for Q_{24} of Rutin

A corresponding increase in the % rutin release of patch was observed with increase in concentrations of Eudragit RL 100. From the Contour plots, 3D surface plots (Figure 10) and the regression coefficient values of all factors, it can be concluded that the Rutin release appeared to increase more with an increasing amount of the Eudragit RL 100 as compared to Eudragit RS 100 and menthol. The more increase in the drug release by Eudragit RL 100 as compared to Eudragit RS 100 could be explained by difference in the permeability characteristics. Eudragit RL 100 is freely permeable to water whereas Eudragit RS 100 is slightly permeable to water. Eudragit RL 100 possesses more ammonium content as compared to the Eudragit RS 100.

For Q_{24} of Rutin, the significance levels of the coefficients b12, b13, b23 and b123 were found to be $P = 0.009387$, 0.5348, 0.1257 and 0.7689 respectively, so they were omitted from the full model to generate a reduced model. The coefficients b1, b2 and b3 were found to be significant at $P < 0.05$; hence they were retained in the reduced model. The reduced model for Q_{24} of rutin,

$Q_{24} = 73.656 + (4.391^* X1) + (0.741^* X2) + (1.396^*X3)$

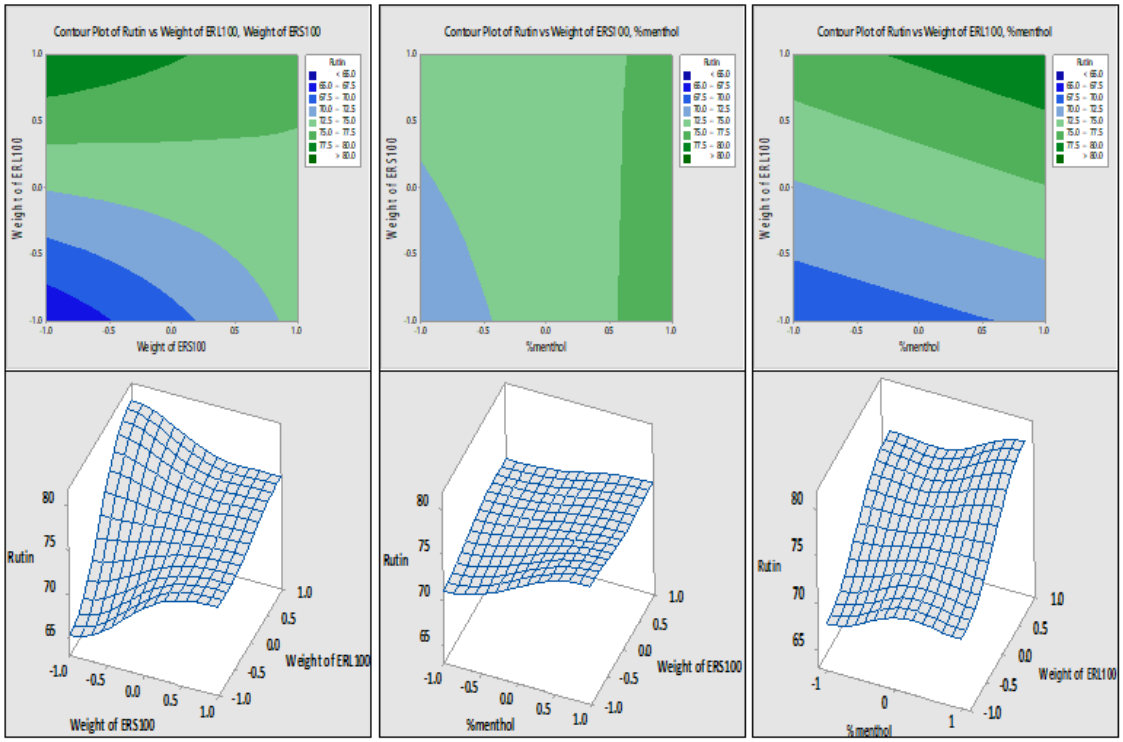

Figure 10: Response surface plot for Q24 of rutin

(A) Effect of weight of ERL 100 (mg) X1 and weight of ERS 100 (mg) X2 on response Y2 (Q24 of rutin) (B) Effect of weight of ERS 100 (mg) X2 and concentration of Menthol (%w/w) X3 on response Y2 (Q24 of rutin) (C) Effect of weight of ERL 100 (mg) X1 and concentration of Menthol (%w/w) X3 on response Y2 (Q24 of rutin)

Ex-vivo skin permeation study of optimized patch

Formulated patch P8 showed maximum Q_{24} for boswellic acids 27.91%, curcuminoids 86.64%, diosgenin 11.57 % and rutin 80.77%. Therefore, it was selected as an optimized batch and studied further for Ex-vivo skin permeation study using Franz diffusion cell. Flux and permeability coefficient (Kp) were shown in Table 12.

Table 12: Ex-vivo skin permeation study of optimized transdermal patch

Time (hr)	Cumulative Percentage drug release			
	Boswellic acids	Curcuminoids	Diosgenin	Rutin
1	1.20	9.60	0.45	7.78
2	3.82	23.41	0.86	22.07
6	9.17	40.28	1.26	40.36
12	18.36	61.76	5.06	60.42
24	29.23	89.26	12.25	84.52
Flux (µg/cm²hr)	0.971	4.18	0.479	4.004
Permeability coefficient, Kp (cm/hr)	0.1941	0.244	0.2158	0.2883

Kinetic modeling of permeation data of optimized patch

The kinetic parameters of skin permeation for optimized batch P8 were presented in Table 13.

Table 13: Kinetic modeling of skin permeation data of optimized patch

Drugs	R^2 Value				N
	Zero order	First order	Higuchi	Korsmeyer-Peppas	
Boswellic acids	0.9719	0.9894	0.8951	0.9931	0.810
Curcuminoids	0.8131	0.9828	0.9789	0.9928	0.585
Diosgenin	0.9633	0.9562	0.7208	0.9928	1.362
Rutin	0.7938	0.9845	0.9746	0.9864	0.577

The zero-order plots for all the drug of batch P8 were found to be linear, as indicated by their high regression values between 0.7938 and 0.9719. Therefore, it was ascertained that the skin permeation of drugs from this formulation could follow zero-order kinetics. Hence, to confirm the exact mechanism of skin permeation from, the data were fitted to the Korsmeyer-Peppas model. In the present study, the coefficient of determination (R^2=0.9864 to 0.9931) was found to be much closer to 1 and the release exponent 'n' value vary between 0.577 to 1.362, which explained that drug released occurs by Non- Fickian type of diffusion. Overall results of kinetic modelling suggest that diffusion is dominant mechanism for drug release following Non-Fickian type of diffusion.

Accelerated stability study of optimized patch

The data of stability studies of optimized batch were summarized in Table 14 -15.

Table 14: Physicochemical parameters of optimized patch after 90 days under accelerated stability testing conditions

Parameters	Result
Thickness (mm)	0.42 ± 0.02
Weight (g/9cm^2)	0.363 ± 0.0227
Folding endurance	80 ± 1.53
% Flatness	99.61 ± 0.248
Tensile Strength	1.53 ± 0.058
% moisture Uptake	4.40 ± 0.66
% moisture Content	3.30 ± 0.08
Water Vapour Transmission Rate (g/cm^{2}24hr)	4.60 ± 0.11
Drug content	
Boswellic acids	99.33
Curcuminoids	99.18
Diosgenin	98.85
Rutin	99.79

*Values are expressed as Mean ± SD (n = 3)

Table 15: In-vitro drug release of optimized patch after 90 days under accelerated stability testing conditions

Time (hr)	Cumulative Percentage drug release			
	Boswellic acids	Curcuminoids	Diosgenin	Rutin
1	0.00	10.65	0.45	8.28
2	2.93	25.25	0.86	19.96
6	8.34	44.20	2.62	35.31
12	17.35	64.51	5.74	56.46
24	27.85	86.31	10.90	80.36

The result of this study showed that drugs remained stable in patch formulation at accelerated conditions for 90 days. No significant variations in drug content and cumulative percent In vitro release of drugs at 24 hr was observed at mentioned conditions.

Primary skin irritation study of formulated herbal transdermal patch

The skin irritation score of erythema and oedema after the application of optimized transdermal patch are shown in Table 16.

Table 16: Skin irritation score following transdermal patch application

Rat No.	Group-I (Normal control)		Group-II (Formalin treated)		Group-III (Non-medicated patch)		Group-IV (formulated patch)	
	Erythema	Edema	Erythema	Edema	Erythema	Edema	Erythema	Edema
1	0	0	3	2	0	0	1	1
2	0	0	3	1	0	0	1	0
3	0	0	3	3	0	0	0	1
4	0	0	3	1	0	0	1	0
5	0	0	2	2	0	0	1	1
6	0	0	3	3	0	0	0	1
PII + SD	0	0	2.83 + 0.41	2.00 + 0.89	0	0	0.67 + 0.52	0.67 + 0.52

Optimized transdermal patch showed a skin irritation score (erythema and edema) of less than 2. According to Draize et al.(2003), compounds producing scores of 2 or less are considered negative (no skin irritation). Hence, developed transdermal patch was not found to cause skin irritation which shows that it is suitable for topical use.

Conclusion

Matrix type polyherbal transdermal patch of boswellic acids, curcuminoids, diosgenin and rutin was prepared by solvent casting method using polymer combination of eudragit RL 100 and eudragit RS 100 and menthol as penetration enhancer. Concentration Polymers and menthol influenced tensile strength and in-vitro drug release. Statistical optimization of 2^3 optimal response surface design proved to be very useful in the subsequent formulation development work following preliminary evaluations. Batch P8, which showed desirable tensile strength and maximum release of drugs at 24 hrs, was selected as an optimized batch. It showed highest % moisture content, % moisture uptake, WVTR and folding endurance. Ex-vivo skin permeation study

and kinetic modelling data of optimized batch explained drug release follow Non-Fickian type of diffusion mechanism. Overall, an optimized, stable and safe polyherbal transdermal patch was successfully developed which could release significant amounts of drugs into the systemic circulation up to 24 hr. Thus, polyherbal patch could be a promising approach for the transdermal delivery of phytochemicals for treatment of arthritis.

Acknowledgements
The authors are thankful to B. K. Mody Government Pharmacy College, Rajkot, Gujarat, India for providing the required facilities and support to complete the present research work. The authors are also thankful to the Department of Pharmacognosy, K. B. Institute of Pharmaceutical Education and Research, Gandhinagar, Gujarat, India for providing HPTLC facility for this research work.

Funding
No funding was obtained for this study.

Statement of Human and Animal Rights
Necessary authorization and endorsement were obtained from the Institutional Animal Ethics Committee (IAEC), B. K. Mody Government Pharmacy College, Rajkot, Gujarat, India, and the Committee for the Purpose of Control and Supervision of Experiments on Animals (CPCSEA), under the Reg. No. BKMGPC/IAEC19/RP29/2017.
This article does not contain any studies with human subjects performed by any of the authors.

Competing interests
The authors declare that they do not have any competing interests.

Conflicts of interest
All authors (R. P. Parmar, N.S. Kanaki) declare that they have no conflicts of interest.

Abbreviations
ABA	3-acetyl β-boswellic acid
AKBA	3-acetyl 11-keto β-boswellic acid
ANOVA	Analysis of Variance
BA	β-boswellic acid
BCS	Biopharmaceutical Classification system
CMC	Carboxy Methyl Cellulose
CPCSEA	Committee for Purpose of Control and Supervision on Experiments on Animals
DMARDs	Disease Modifying Anti-Rheumatic Drugs
DSC	Differential Scanning Calorimeter
EC	Ethyl Cellulose
ERL 100	Eudragit RL 100
ERS 100	Eudragit RS 100
FDC	Franz Diffusion cell
FM	Full Model
FTIR	Fourier Transform Infrared
HPC	Hydroxy Propyl Cellulose
HPMC	Hydroxy Propyl Methyl Cellulose
HPTLC	High Performance Thin Layer chromatography

IAEC	Institutional Animal Ethics Committee
KBA	11-keto β-boswellic acid
Kp	Permeability coefficient
MC	Moisture Content
MU	Moisture Uptake
NDDS	Novel Drug Delivery System
NSAIDs	Non-Steroidal Anti-inflammatory Drugs
PBS	Phosphate Buffer Solution PBS
PEG	Polyethylene Glycol
PG	Propylene Glycol
PDII	Primary Dermal Irritation Index
PVP K30	Poly Vinyl Pyrrolidine K30
Q24	% cumulative drug release at 24 hr
RA	Rheumatoid Arthritis
RH	Relative humidity
RM	Reduced Model
SD	Standard Deviation
SPI	Score of Primary Irritation
TDDS	Transdermal Drug delivery System
WVTR	Water Vapor Transmission Rate

References

1. Ammon, H.P., Safayhi, H., Mack, T. and Sabieraj, J. (1993). Mechanism of anti-inflammatory actions of curcumine and boswellic acids. J Ethnopharmacol. 38 (2-3), 105-112. DOI: https://doi.org/10.1016/0378-8741(93)90005-P
2. Basar S. (2005) Phytochemical investigations on Boswellia species. PhD thesis, Hamburg.
3. Draize, J.H., Woodard, G. and Calvery, H.O. (1944). Methods for the study of irritation and toxicity of substances applied topically to the skin and mucous membranes. J Pharmacolo Exp Ther. 82 (3), 377-390. Link: https://jpet.aspetjournals.org/content/82/3/377
4. Fartyal, S., Jha, S.K., Gupta, R., Vajpayee, A. and Karchuli, M.S. (2011) Formulation and evaluation of floating microspheres of boswellic acid. Int J PharmTech Res. 3(1), 76-81.
5. Ganeshpurkar, A. and Saluja, A.K. (2016) The Pharmacological Potential of Rutin. Saudi Pharmaceutical J. 25 (2), 149-164. DOI: http://dx.doi.org/10.1016/j.jsps.2016.04.025
6. Ayurvedic Pharmacopoeia of India Part I. Vol. 1. Government of India, New Delhi; 1999. Haridra: 60-61.
7. Ayurvedic Pharmacopoeia of India part I. Vol. 4. Government of India, New Delhi; 1999. Kunduru: 57-58.
8. Hatcher, H., Planalp, R., Chob, J., Torti, F.M. and Torti, S.V. (2008) Curcumin: From ancient medicine to current clinical trials. Cell. Mol. Life Sci. 65 (11), 1631-1652.
9. DOI: http://dx.doi.org/10.1007/s00018-008-7452-4.
10. Indian Herbal Pharmacopoeia. Vol. 1. A joint publication of Regional Research Laboratory, Jammu and Indian Drug Manufacturers' Association, Mumbai; 1998. Turmeric: 64-72.
11. Indrayanto, G., Utami, W., Santosa, M.H. and Syahrani, A. (1994) Analytical profiles of drug substances and excipients. 23, 99- 124.
12. Jain, S., Vaidya, A., Gupta, P.K., Rosenholm, J.M. and Bansal, K.K. (2021) Antiarthritic activities of herbal isolates: A comprehensive review. Coatings. 11 (11), 1329.
13. DOI: https://doi.org/10.3390/coatings11111329

14. Javed, M., Saleem, A. and Akhtar, M.F. (2023) Diosgenin, a steroidal sapogenin, arrests arthritis through modulation of inflammatory cytokines and oxidative stress biomarkers in Wistar rats. Inflammopharmacology. 31(4), 1951–1966.
15. DOI: https://doi.org/10.1007/s10787-023-01244-7
16. Khanna, D., Sethi, G., Ahn, K.S., Pandey, M.K., Kunnumakkara, A.B., Sung, B., Aggarwal, A. and Aggarwal, B.B. (2007) Natural products as a gold mine for arthritis treatment. Current Opinion in Pharmacology. 7, 344– 351. DOI: https://doi.org/10.1016/j.coph.2007.03.002
17. Liu, Cz., Chang, Jh., Zhang, L., Xue, Hf., Liu, Xg., Liu, P. and Fu, Q. (2017) Preparation and evaluation of diosgenin nanocrystals to improve oral bioavailability. AAPS PharmSciTech 2017; 18(6): 2067–2076. DOI: https://doi.org/10.1208/s12249-016-0684-y
18. Mohan, P.R., Sreelakshmi, G., Muraleedharan, C.V. and Joseph, R. (2012) Water soluble complexes of curcumin with cyclodextrins: Characterization by FT-Raman spectroscopy. Vib Spectrosc. 62, 77– 84. DOI: https://doi.org/10.1016/j.vibspec.2012.05.002
19. Mrid, R.B., Bouchmaa, N., Ainani, H., Fatimy, R.E., Malka, G. and Mazini, L. (2022) Anti-rheumatoid drugs advancements: new insights into the molecular treatment of rheumatoid arthritis. Biomedicine and Pharmacotherapy. 151, 113–126.
20. Panhwar, Q.K. and Memon, S. (2014) Synthesis, characterization and antioxidant activity of rutin complexes. Pak J Anal Environ Chem. 15(2), 60– 70.
21. Parmar, R.P. and Kanaki N.S. (2017) Development of HPTLC Method for estimation of rutin in polyherbal transdermal gel. World journal of pharmacy and pharmaceutical sciences. 6(9), 1188– 1194. DOI: https://doi.org/10.20959/wjpps20179-9983
22. Parmar, R.P. and Kanaki N.S. (2018). Development of Simultaneous HPTLC Method for estimation of boswellic acid, curcumin and diosgenin in polyherbal transdermal gel.
23. Res. J. Pharmacognosy and Phytochem. 10 (2), 163–167.
24. DOI: https://doi.org/10.5958/0975-4385.2018.00024.9
25. Patel, K., Gadewar, M., Tahilyani, V. and Patel D.K. (2012) A review on pharmacological and analytical aspects of diosgenin: a concise report. Nat. Prod. Bioprospect. 2, 46–52.
26. DOI: https://doi.org/10.1007/s13659-012-0014-3.
27. Patel, N.A., Patel, N.J. and Patel, R.P. (2009) Design and evaluation of transdermal drug delivery system for curcumin as an anti-inflammatory drug. Drug Dev Ind Pharm. 35(2), 234–242. DOI: https://doi.org/10.1080/03639040802266782
28. Prabhakar, D., Sreekanth, J. and Jayaveera, K.N. (2013) Transdermal drug delivery patches: A review. Journal of Drug Delivery and Therapeutics 3(4), 213–221.
29. DOI: https://doi.org/10.22270/jddt.v3i4.590
30. Prausnitz, M. and Langer, R. (2008) Transdermal drug delivery. Nat Biotechno. 26, 1261–1268. DOI: https://doi.org/10.1038/nbt.1504
31. Rao, M., Sonavane, V., Kulkarni, S., Magar, M., Zope, A., & Karanjkar, P. (2019). Design of transdermal patch of ketoprofen by full factorial design for treatment of rheumatoid arthritis. Journal of Drug Delivery and Therapeutics, 9(2), 197–205.
32. DOI: http://dx.doi.org/10.22270/jddt.v9i2.2549
33. Ravi, G.S., Charyulu, R.N., Dubey, A., Prabhu, P., Hebbar, S. and Mathias, A.C. (2018) Nano-lipid complex of rutin: Development, characterization and In-vivo investigation of hepatoprotective, antioxidant activity and bioavailability study in rats. AAPS PharmSciTech, 19(8), 3631–3649. DOI: https://doi.org/10.1208/s12249-018-1195-9
34. Revathy, S.S., Elumalai, S., Benny, M. and Antony, B. (2011) Isolation, purification and identification of curcuminoids from turmeric (Curcuma longa L.) by column chromatography. J Exp Sci. 2(7), 21–25.

35. Roy, J. "An Introduction to Pharmaceutical Sciences" New pharmaceutical technology and pharmaceuticals, Woodhead Publishing Limited: 349-356
36. Scott, D.L., Wolfe, F. and Huizinga, T.W.J. (2010) Rheumatoid arthritis. Lancet. 376 (9746), 1094-1108. DOI: https://doi.org/10.1016/S0140-6736(10)60826-4
37. Sharma, M.L., Bani, S. and Singh, G.B. (1989) Anti-arthritic activity of boswellic acids in bovine serum albumin (BSA)-induced arthritis. Int J Immunopharmacol. 11(6), 647-652. DOI: https://doi.org/10.1016/0192-0561(89)90150-1
38. Smolen, J.S., Aletaha, D. and McInnes, I.B. (2016) Rheumatoid arthritis. Lancet. 388 (10055), 2023-2038. DOI: https://doi.org/10.1016/S0140-6736(16)30173-8
39. Srivastava C. (2009) Phytochemistry and medicobotany of some medicinal plants used in treatment of arthritis. Medicinal Plants - International Journal of Phytomedicines and Related Industries. 1(1), 27-32. DOI: https://doi.org/10.1016/S0140-6736(10)60826-4
40. Tonnesen, H.H., Masson, M. and Loftsson, T. (2002) Studies of curcumin and curcuminoids XXVII. Cyclodextrin complexation: Solubility, chemical and photochemical stability. Int. J. Pharm. 244(1-2), 127-135. DOI: https://doi.org/10.1016/S0378-5173(02)00323-X
41. Varia, U., Joshi, D., Jadeja, M., Katariya, H. and Detholia, K. (2022) Development and evaluation of ultradeformable vesicles loaded transdermal film of boswellic acid. Future Journal of Pharmaceutical Sciences. 8: 39. DOI: https://doi.org/10.1186/s43094-022-00428-2

Figure legend

Figure 1: Chemical structure of boswellic acid, curcumin, diosgenin and rutin
Figure 2: HPTLC chromatogram and calibration curve of standard boswellic acids and diosgenin in methanol
Figure 3: HPTLC chromatogram and calibration curve of standard curcuminoids and rutin in methanol
Figure 4: Calibration curve of boswellic acid, curcuminoids, diosgenin and rutin in diffusion medium by HPTLC
Figure 5: Cumulative percentage release of boswellic acids, curcuminoids, diosgenin and rutin from factorial design batches of transdermal patch
Figure 6: Response surface plot for Tensile strength
Figure 7: Response surface plot for Q24 of boswellic acids
Figure 8: Response surface plot for Q24 of curcuminoids
Figure 9: Response surface plot for Q24 of diosgenin
Figure 10: Response surface plot for Q24 of rutin

Table legend

Table 1: Design layout for 2^3 full factorial batches of transdermal patch
Table 2: Groups and treatments for skin irritation study
Table 3: Classification system for skin reactions
Table 4: Response categories of irritations in rats
Table 5: FTIR study of drugs and excipients
Table 6: Compatibility studies of drug and polymer by DSC thermograms
Table 7: Experimental runs and measured responses of 2^3 full factorial design batches of transdermal patch
Table 8: Result of evaluation parameters of 2^3 full factorial design batches of transdermal patch
Table 9: Result of evaluation parameters of 2^3 full factorial design batches of transdermal patch